2016

ENHANCEMENT OF MARGRAVE DECONVOLUTION AND Q ESTIMATION IN HIGHLY ATTENUATING MEDIA USING THE MODIFIED S-TRANSFORM

Adnan Djeffal
Michigan Technological University, adjeffal@mtu.edu

ENHANCEMENT OF MARGRAVE DECONVOLUTION AND Q ESTIMATION IN HIGHLY ATTENUATING MEDIA USING THE MODIFIED S-TRANSFORM

By

Adnan Djeffal

A THESIS

Submitted in partial fulfillment of the requirements for the degree of

MASTER OF SCIENCE

In Geophysics

MICHIGAN TECHNOLOGICAL UNIVERSITY

2016

This thesis has been approved in partial fulfillment of the requirements for the Degree of MASTER OF SCIENCE in Geophysics.

Department of Geological and Mining Engineering and Sciences

Thesis Co-Advisor: *Dr. Wayne D. Pennington*

Thesis Co-Advisor: *Dr. Roohollah Askari*

Committee Member: *Dr. Roger M. Turpening*

Department Chair: *Dr. John S. Gierke*

Table of Contents

Acknowledgements

First, I would like to thank Dr. Roohollah Askari and Dr. Wayne D. Pennington. Without their guidance, support, useful critiques and patience over the past year, this thesis would not have been possible.

I also appreciate the guidance provided by Dr. Roger M. Turpening, who oversaw the croseewell seismic data collection in Michigan, and who provided the data for this project.

Thank you to the Fulbright Program for giving me a valuable opportunity to experience a different culture while pursuing graduate studies. Thank you to the AMIDEAST staff for their support over the past two years.

I would like also to thank CREWES, the research group at the University of Calgary, for their open source Matlab toolbox that was used extensively in this research.

I would like to express my appreciation to my friends for their encouragements.

Most importantly, I deeply thank my parents, brothers and sisters for their understanding and emotional support. I love you all.

Abstract

We evaluate the performance of the Margrave deconvolution and spectral ratio methods using the Gabor, S-, and modified S transforms in highly attenuating media, where the quality factor changes with depth dramatically. Our results substantiate that the modified S-transform deconvolution is more robust in terms of generating fewer artifacts and providing better estimates of reflectivities than the Gabor transform. The results also show that using the modified S-transform in the spectral ratio method produces better Q estimates than the S-transform and the Fourier transform that is conventionally used in the spectral ratio method. This improvement in the estimates of reflectivities and Q using the modified S-transform is due to the enhancement of the time-frequency decomposition obtained by substituting the frequency in the Gaussian window with a linear frequency function. The coefficients of this linear function control the time frequency localization by expanding the Gaussian window at low frequencies and tightening it at high frequencies, in turn providing a better time-frequency decomposition. We demonstrate the efficiency of the modified S-transform deconvolution and Q estimation through the analysis of both synthetic and field data.

1. Introduction

Seismic deconvolution increases the temporal resolution, suppresses multiples, and yields some approximations of reflectivities (Yilmaz, 2001). The assumptions often used in conventional deconvolution techniques include a minimum phase wavelet, nonstationarity of the seismic signal, white spectrum reflectivity model, noise-free seismogram, normal incidence condition, and flatness of geological layers (Yilmaz, 2001). In addition, the seismic wavelet is assumed to be solved for using various criteria. However, in the real world, most of the mentioned conditions are not satisfied, in particular, the non-stationarity of seismic signal as the frequency content of seismic signal changes with time (Askari and Siahkoohi, 2008).

Margrave et al. (2002) proposed a nonstationary deconvolution model using the Gabor transform (Gabor, 1946). In their methodology, the quality factor is assumed to be constant. In the time-frequency domain, Margrave et al. (2002) estimate the seismic wavelet amplitude spectrum by simply smoothing the amplitude spectrum of the Gabor transform of a seismic signal by convolving over time and frequency using a 2-D boxcar. Considering a minimum-phase assumption, the phase spectrum of the wavelet in the Gabor transform domain is calculated from its amplitude spectrum previously estimated. As a result of these assumptions – mainly that the phase and amplitude spectra of a seismic wavelet are known – the phase and amplitude spectra of the reflectivity series can be calculated in the Gabor transform domain, and then transformed back into the time domain (Margrave et al., 2002).

Margrave et al. (2011) improved their deconvolution model using a set of windows that forms partition of unity (POU). Todorov and Margrave (2009) used the S-transform (Stockwell et al., 1996; Stockwell, 2006) for the deconvolution instead of the Gabor transform. They concluded that the S-transform improved the reflectivity estimate of the Margrave deconvolution. Radad et al. (2015) introduced the S-transform with maximum energy concentration, and applied it to the Margrave deconvolution. Their method provided a better estimate of reflectivities compared to the conventional S-transform and the Gabor transform.

In general, Margrave deconvolution based on the Gabor transform provides reasonable estimates of the reflectivity series when the quality factor is high and constant. However, for a geological model where the quality factor is low and dramatically varies with depth, the Margrave's Gabor transform-based deconvolution generates some high frequency artifacts that might be mistaken as components of the reflectivity series. The main reason for the poor results of the Gabor deconvolution is an inherent spectral resolution problem

of the Gabor transform: at high frequencies it provides weak time resolution, and at low frequencies it provides low frequency resolution. In this thesis, we present the idea of the Margrave deconvolution in the modified S-transform domain. The modified S-transform improves the time-frequency resolution by replacing the frequency in the Gaussian window with a linear frequency function whose coefficients control the time-frequency resolution at low and high frequencies. We show that for a low quality factor, and also for a time-varying quality factor, the modified S-transform provides more reasonable results than the Gabor and S-transforms.

We also utilize the S- and modified S transforms to estimate Q using the spectral ratio method that traditionally has been based on the Fourier transform (Tonn, 1991). We chose the spectral ratio over other frequency-based methods such as spectral modelling (Jannsen et al., 1985) because it is the most frequently used tool for estimating the quality factor, Q, in the field and laboratory (Mavko et al., 2009). Reine et al. (2009) compared four spectral decomposition methods used in the spectral ratio applications. They concluded that the spectral decomposition methods with a length-varying window such as the S-transform yielded more accurate estimates of Q than the methods that utilize a fixed-length window such as Gabor transform. Du et al. (2010) used the S-transform with regularized inversion to estimate Q. Their regularized inversion produced a smoother ratio over the regular division therefore the estimated values of Q were more robust.

In this thesis, we apply the Fourier, S- and modified S transforms to compute the ratio of trace spectra at travel time t_1 and t_2.Then, we estimate Q from the slope by assuming a straight-line relationship. We show through synthetic traces and real data that the modified S-transform produces better estimates of Q in highly attenuating media because of its linear function allowing more control of the window length.

2. Theory

2.1 Gabor Transform

Gabor (1946) proposed the Short Time Fourier method known as Gabor transform to localize the frequency and time distribution of nonstationary signals

$$G(\tau, f) = \int_{-\infty}^{+\infty} h(t)w(t-\tau)e^{-i2\pi ft}\,dt \tag{1}$$

where $h(t)$ is a signal, $w(t)$ is the analysis window and $G(\tau, f)$ is the complex Gabor spectrum. In practice, the analysis window is usually a Gaussian window that is used to localize the time-frequency spectra. The fixed length of the window produces a low resolution of the time-frequency localization. A wide window leads to a high frequency resolution but at the cost of low time resolution, and vice versa. This tradeoff is also known as Heisenberg's uncertainty principle (Heisenberg, 1927).

2.2 S-Transform

Stockwell et. al (1996) introduced the S-transform defined as

$$S(\tau, f) = \int_{-\infty}^{+\infty} h(t)\left[\frac{|f|}{\sqrt{2\pi}} e^{\frac{-(\tau-t)^2 f^2}{2}}\right] e^{-i2\pi ft} dt. \tag{2}$$

The term in the bracket is the Gaussian window scaled by frequency. Because of the scalability of the Gaussian window in the S-transform, the S-transform improves the time-frequency resolution. In addition, by applying different parameters in the Gaussian window, we yield different versions of the S-transform that are termed the generalized S-transform in the literature (Askari and Ferguson, 2012).

2.3 Modified S-Transform

Li and Castagna (2013) introduced a new version of the S-transform by replacing the frequency in the Gaussian window by a linear frequency function. The Modified S-transform (Li and Castagna, 2013) is given by

$$S(\tau, f) = \int_{-\infty}^{+\infty} h(t) \frac{\alpha|f|+\beta}{\sqrt{2\pi}} e^{\frac{-(\tau-t)^2(\alpha|f|+\beta)^2}{2}} e^{-i2\pi f t} dt \qquad (3)$$

where α and β are the coefficients of the linear function, $\alpha|f| + \beta$. The linear frequency function extends the Gaussian window more at low frequencies and contracts it more at high frequencies (Askari and Hejazi, 2015). Thus, the modified S-transform provides a better time frequency resolution over the S-transform.

We applied the Gabor transform (Figure 1b), the S-transform (Figure 1c) and the modified S-transform (Figure 1d) to the chirp in Figure 1a. The modified S-transform provides a better time resolution at low frequencies and frequency resolution at high frequencies in comparison with the conventional S-transform and the Gabor transform.

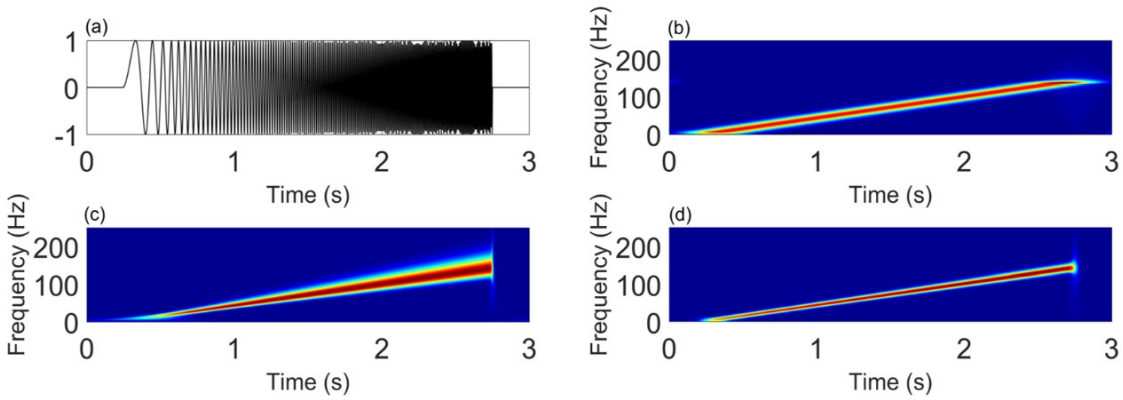

Figure 1. (a) A chirp whose frequency increases with time, (b) Gabor spectrum, (c) S-transform spectrum and (d) Modified S-transform spectrum

2.4 Margrave Deconvolution Using the Modified S-Transform

We use the modified S-transform to improve the Margrave deconvolution (Margrave et al., 2002). We follow the same procedure used by Margrave et. al (2002) with the Gabor transform to obtain the Margrave deconvolution with the modified S-transform domain.

The nonstationary trace model in the Margrave deconvolution is defined as

$$S(f) = W(f) \int_{-\infty}^{+\infty} \alpha_Q(\tau, f) r(\tau) e^{-2\pi i f \tau} d\tau \tag{4}$$

where S and W are the nonstationary seismic trace and the source signature respectively. $\int_{-\infty}^{+\infty} \alpha_Q(\tau, f) r(\tau) d\tau$ is the nonstationary convolution filter defined by Margrave (1998). The model is expressed in the Fourier domain for simplicity.

Margrave et. al (2002) proved that applying the Gabor transform to the convolution filter model in Equation (4) is equal to the product of the Fourier transform of the source signature, the constant quality factor, Q, transfer function, and the Gabor transform of the reflectivity as expressed in equation (5).

$$V_g s(\tau, f) \approx W(f) \alpha_Q(\tau, f) V_g r(\tau, f) \tag{5}$$

where $V_g s(\tau, f)$ and $V_g r(\tau, f)$ are the Gabor transform of the nonstationary trace and reflectivities respectively. Smoothing the amplitude spectrum in the Gabor transform of the nonstationary trace gives an estimate of the amplitude spectrum in the Gabor transform of $W(f)\alpha_Q(\tau, f)$. The smoother can be of different shapes, for example: a 2-D box car, Gaussian or hyperbolic. Considering a minimum phase assumption, the phase spectrum of the wavelet in the Gabor transform domain is calculated from the estimated amplitude spectrum of $W(f)\alpha_Q(\tau, f)$.

Thus, the reflectivity in the Gabor domain is expressed as

$$V_g r(\tau, f) = \frac{V_g s(\tau, f)}{|V_g s(\tau, f)|_{est}} e^{-i\varphi(\tau, f)} \tag{6}$$

where $|V_g s(\tau, f)|_{est}$ is the estimated amplitude spectrum of $W(f)\alpha_Q(\tau, f)$. Finally, the reflectivities are obtained by calculating the inverse of Gabor transform.

In this study, in addition to the Gabor transform, we utilize the S-transform and modified S-transform to evaluate the performance of the Margrave deconvolution in a highly attenuating medium.

2.5 Spectral Ratio

Du et al. (2010) defined the amplitude spectrum of a signal in a homogeneous attenuating medium as

$$S(f, t) = A(t) S(f, t_0) e^{-\frac{\pi f}{Qv} z} \tag{7}$$

where f is the frequency, $S(f, t)$ is the signal amplitude spectrum after propagating a certain disrance z, $S(f, t_0)$ is the ampltiude spectrum of the signal at t_0 and $A(t)$ is a factor independent of frequency. At travel time t_1 and t_2, we obtain

$$S(f, t_1) = A(t_1) S(f, t_0) e^{-\frac{\pi f}{Q} t_1} \tag{8}$$

and

$$S(f, t_2) = A(t_2) S(f, t_0) e^{-\frac{\pi f}{Q} t_2} \tag{9}$$

Dividing equation (9) by equation (8), we obtain

$$\frac{S(f,t_2)}{S(f,t_1)} = \frac{A(t_2)e^{-\frac{\pi f}{Q}t_2}}{A(t_1)e^{-\frac{\pi f}{Q}t_1}} \tag{10}$$

The quality factor , Q, is deducted by taking the natural logs of both sides of equation (10)

$$\ln\left[\frac{S(f,t_2)}{S(f,t_1)}\right] = C - \frac{\pi f(t_2-t_1)}{Q} \tag{11}$$

We determine Q from the slope by assuming a straight-line relationship. The Q estimated counts for intrinsic effects such as fluid flow and apparent attenuation effects such as multiple scattering (Spencer et al., 1982).

In this study, we compute the amplitude spectrum of the signal using the S- and modified S transforms in addition to the Fourier transform and we compare the estimated values of Q from the three decompositional methods.

3. Deconvolution Results and Discussion

3.1 Synthetic Data Deconvolution

To evaluate Margrave's deconvolution using the Gabor, S-, and the modified S- transforms, we consider two synthetic traces respectively with the quality factors of 100 and 30 and the wavelet dominant frequencies of 25 Hz and 50 Hz (Figures 2a and 3a). The time sampling is 2ms. The three deconvolution methods were applied to the synthetic traces.

Figures 2c-e and Figure 3c-e shows the Margrave deconvolution results of the Gabor transform, S-transform and modified S-transform respectively. In the case of low attenuation (Figure 2) and also in high attenuation (Figure 3), the modified S-transform deconvolution outperformed the S-transform and Gabor transform deconvolutions. It is evident that in both cases the Gabor transform deconvolution has generated some artifacts as seen in box (1) in Figure 2, and in boxes (1) and (3) in Figure 3. However, the reflectivities artifacts are more noticeable in the highly attenuated trace (Figure 3).

The modified S-transform improved the temporal resolution over the S-transform as seen in box (2) in Figure 3 because of the higher resolution of the time-frequency decomposition.

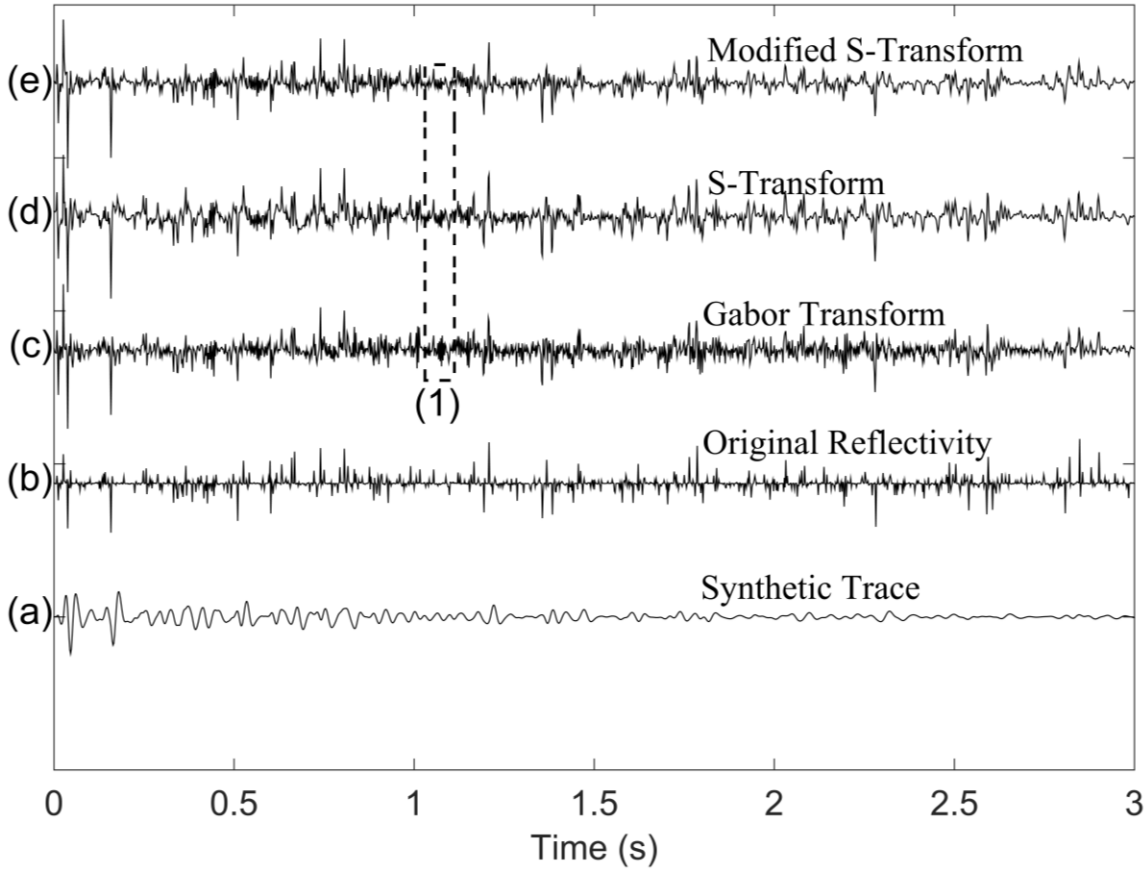

Figure 2. (a) the synthetic trace (dominant frequency =25 Hz, Q = 100); (b) the original reflectivity; and the estimated reflectivity series from Margrave deconvolution using (c) Gabor transform, (d) S-transform and (e) Modified S-transform. Even when the attenuation is low, the Gabor transform generates some artifacts (particularly noticeable in the highlighted area)

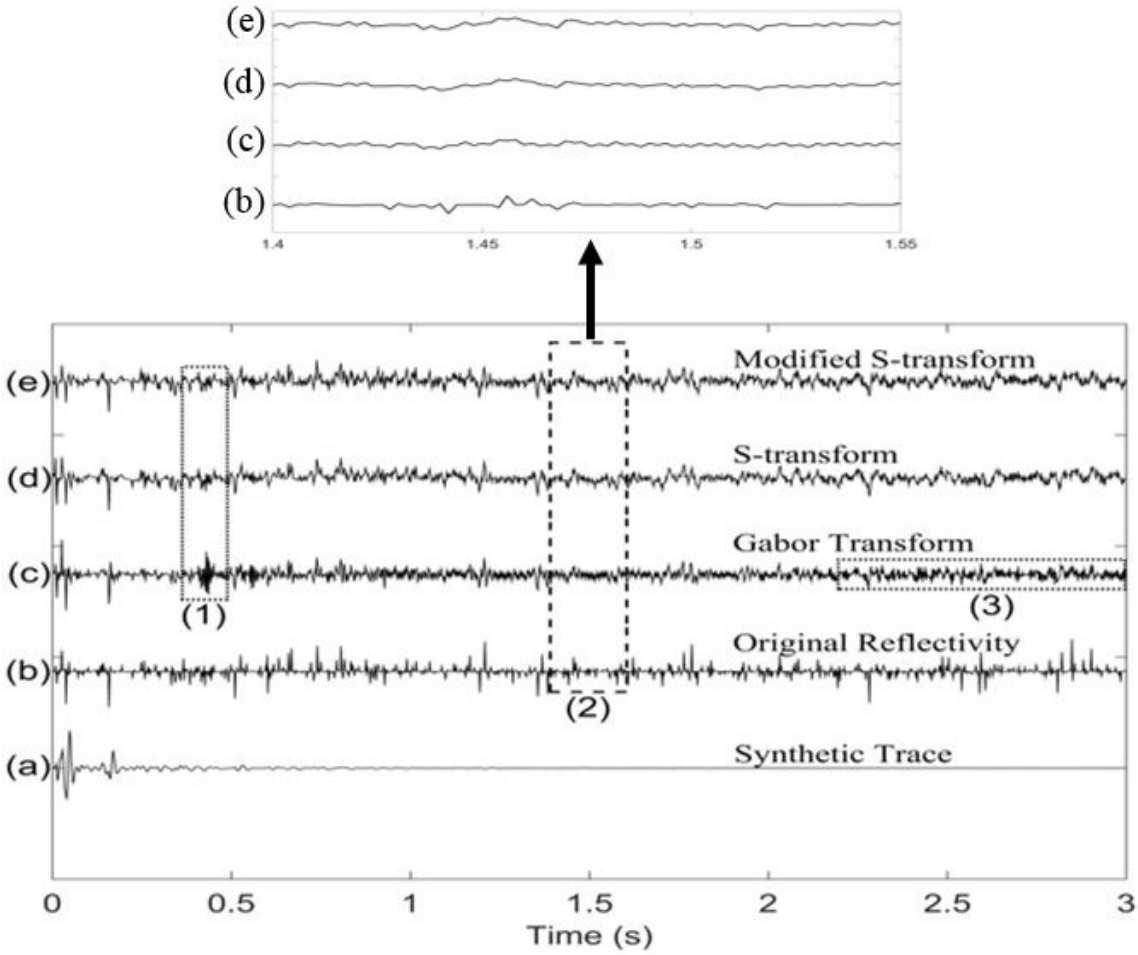

Figure 3. (a) the synthetic signal (dominant frequency =50 Hz, Q = 30), (b) the original reflectivity and the estimated reflectivity of the Margrave deconvolution of (c) Gabor transform, (d) S-transform and (e) modified S-transform. The modified S-transform outperforms the Gabor transform and S-transform. Some areas are highlighted for comparison and referenced in the text. Artifacts generated by the Gabor deconvolution are noticeable.

3.2 Real Data Deconvolution

We study a post-stack cross-well seismic data set of a gas bearing reservoir in Grand Traverse County, Michigan. The objective of this data acquisition was to obtain a high resolution image of a Silurian (Niagaran) reef complex at a depth approximately 5000 ft. In the previous studies, three internal layers and zones within the reef, also known to geologists as lithofacies, have been identified (Ibrahim et al., 2010). The sources were piezoelectric transducers that generate a seismic pulse. The frequency band chosen for this survey went up to 3000 Hz. Due to the high frequency nature of this data set a high resolution velocity model is required for comparable imaging quality, and the conventional seismic processing ended up degrading the resolution of the final image to about 600-700 Hz after stacking. Here, we aim to increase the bandwidth of the data by applying the Margrave deconvolution. However, due to the high attenuation of seismic data, poor pre-stack processing, and depth varying quality factor, we find out that applying the Margrave deconvolution using the Gabor transform generates some artifacts.

Figure 4a shows the seismic image of the crosswell data where the reef location has been highlighted by a yellow box. In the reef, the amplitudes of these reflectors are extremely low. This can be attributed to either attenuation of signal as it passes through the gas saturated reef or a poor velocity model.

Figures 4.b-d show the results of the Margrave deconvolutions using the Gabor (b), S- (c), and modified S- (d) transforms. The comparison of the results shows that the modified S-transform provides better spatial and temporal resolutions than the Gabor and S-transform deconvolutions. The Gabor transform deconvolution has generated lot of artifacts in the reef region that can be mistaken for reflectivities.

To better demonstrate these artifacts, we present a trace in Figure 5a that passes through the reef with its Margrave deconvolution results by the Gabor, S- and modified S transforms as shown in Figures 5-b, 5-c and 5-d respectively. The artifacts are easily noticeable in Gabor's transform's estimate as seen in boxes (2) and (3). The modified S-transform reflectivities estimate produced better spatial and temporal resolution than the S-transform estimate as seen in box (1).

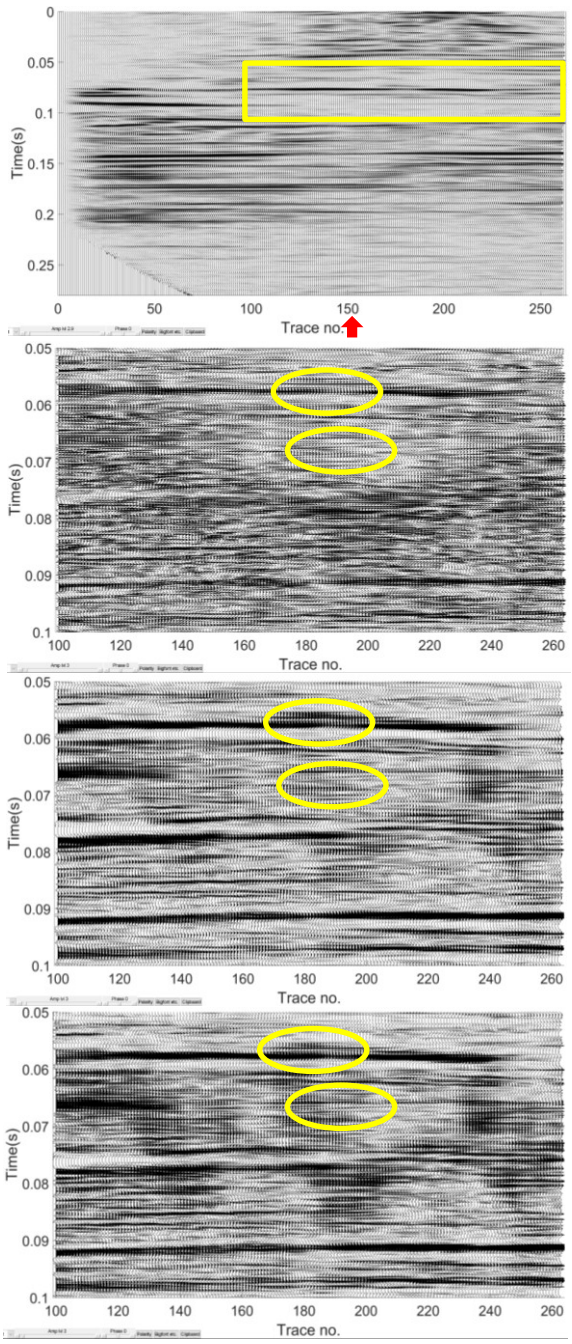

Figure 4. (a) Original reflection-seismic section. The area of interest is the attenuated zone in the yellow box; the Margrave deconvolution results by (b) the Gabor transform, (c) the S-transform, and (d) the modified S-transform.

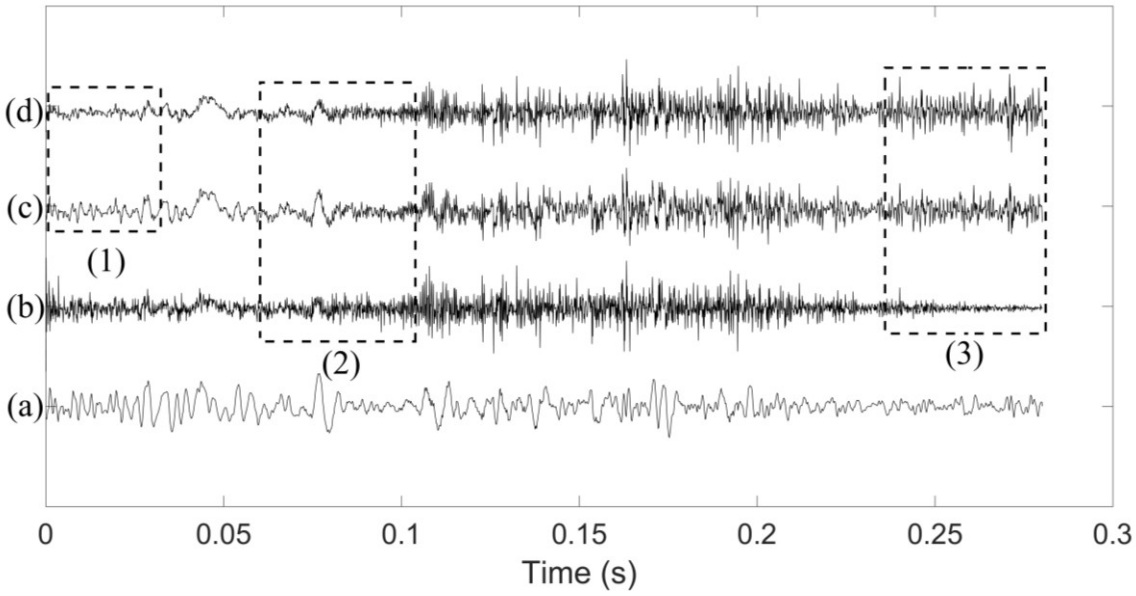

Figure 5. (a) Trace 150 from crosswell data set that passes through the reef (indicated by a red arrow in figure 4.). The Margrave deconvolution results by (b) the Gabor transform, (c) the S-transform, and (d) the modified S-transform.

4. Q Estimation Results and Discussion

4.1 Q from Synthetic Data

To compare the performance of the S-transform and modified S-transform in estimating Q using the spectral ratio method, we consider two synthetic traces with a time sampling of 2ms and dominant frequencies of 30 Hz and 60 Hz. We apply a quality factor of 20 and 50 to each trace to simulate a highly and a moderately attenuating medium respectively. Figure 6-7 show the results of estimating Q using the spectral ratio with the three time-frequency representation methods. The results are summurized in Table (1).

Table 1. The spectral ratio Q estimation results for the modified S-transform, S-transform and Fourier transform.

	Dominant frequency = 30 Hz		Dominant frequency = 60 Hz	
Initial Q	Q=20	Q=50	Q=20	Q=50
Modified S-transform estimates	21	51	22	52
S-transform estimates	21	55	21	54
Fourier transform estimates	18	44	27	42

The estimated Q values in Table (1) are most accurate when a spectral decomposition method with a time-varying window is used. The modified S-transform performed better than the S-transform for both traces when the quality factor is equal to 50. They produced similar results for both traces when the quality factor is equal to 20. However, they both outperformed the Fourier transform conventionally used in the spectral ratio method. The results also demonstrate the huge inaccuracy in estimating Q using the Fourier transform in the case of high frequency traces.

The modified S-transform yielded better estimates of Q because its linear function allows better control over the window length by shortening it in high frequencies and expanding it in low frequencies, which leads to better frequency localization with time. However, the Fourier transform produced poor results because it only informs on the general frequency content of the trace.

4.2 Q from Real Data

To evaluate the spectral ratio method with the Fourier, S- and modified S transforms, we use the same crosswell seismic data of gas-bearing reef acquired in Michigan. We estimated Q in the reef region (0.07s - 0.15s) as well as above (0s - 0.07s) and below (0.15s - 0.28s) it for two traces, 125 and 150. Figure 8 and 9 show the results of the estimated Q using the spectral ratio with the three time-frequency representation methods. The results are summurized in Table (2).

Table 2. The spectral ratio Q estimation results for the modified S-transform, S-transform and Fourier transform.

	Trace 125			Trace 150		
	Above the reef	Within the reef	Below the reef	Above the reef	Within the reef	Below the reef
Modified S-transform estimates	66	39	72	61	37	85
S-transform estimates	54	38	81	61	29	75
Fourier transform estimates	35	86	35	15	53	28

The estimated values for Q from the S- and modified S transforms correlate well with the Q-distribution image of the same crosswell survey developped by Carrilo et al. in 2007 using the centroid frequency shift method. The Q-dstribution image suggests that the section above the reef exhibits minimal attenuation (larger values of Q) than other areas. Whereas, the reef region exhibits very high attenuation (low values of Q). However, the Q estimates from the spectral ratio methods using the Fourier transform failed to correspond to the trend in the Q-distribution image.

The reliability of the Q estimates in Table 2 is dependant on the best fit line that is chosen within a frequency band where the signal standsout. From Figure 8 and 9, we see that the best fit line goes through a rather noisy spectral ratio rendering the accuracy of the Q estimates questionable. Hence, further attenuation studies are need to confirm their validity.

However, checking the validity of the Q values presented in Table 2 is a challenging task because seismic attenuation is a complex phenomena that can be associated to many causes such as intrinsic effects. These effects can be anelastic losses resulting from fluid movements and frictions between grains (Spencer et al., 1982). Also, energy loss can occur from other effects that mimic those of interinc such as multiple scattering (Spencer et al., 1982). Therefore, seperating these effects and associating an independent value of Q to each of them is not a straight forward process.

(a)

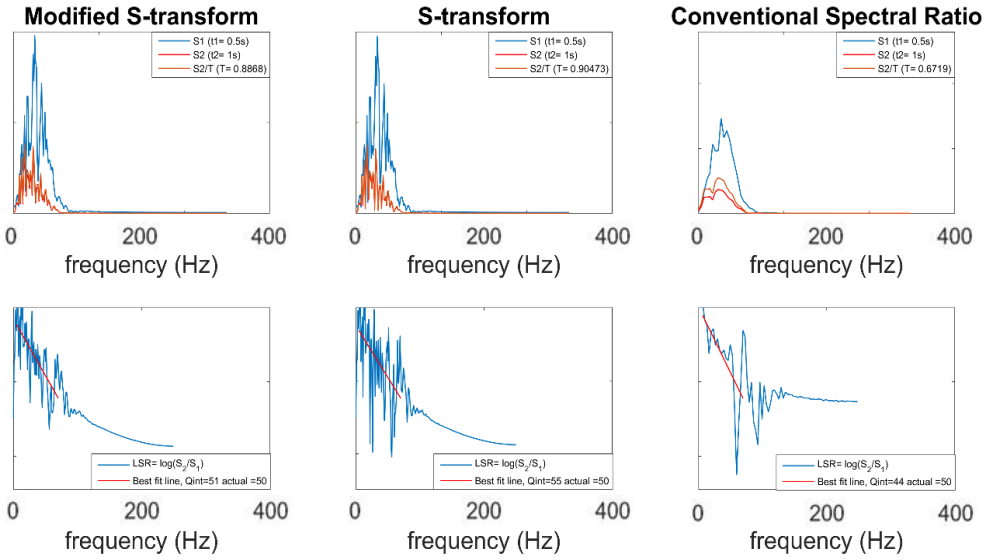

(b)

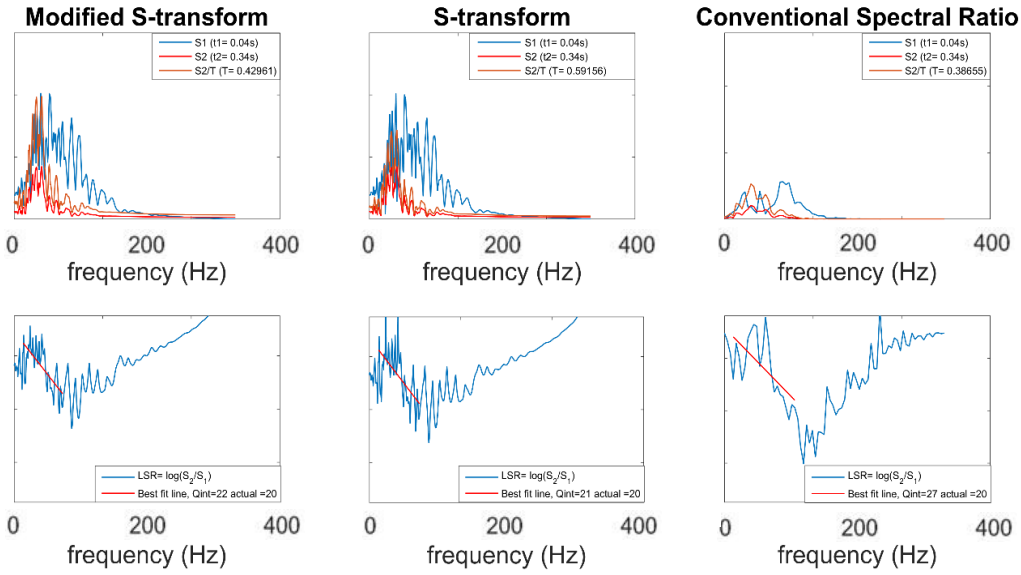

Figure 6. Q estimation for two synthetic traces using the spectral ratio method with the modified S-transform, S-transform and Fourier transform. (a) Q estimation for a synthetic trace with a dominant frequency of 30 Hz and an initial Q of 20 and (b) Q estimation for a synthetic trace with a dominant frequency of 30 Hz and an initial Q of 50. The upper plots are the frequency spectra of the trace at t_1 (blue) and at t_2 (red). The lower plots are the division results of the trace spectrum at t_2 over the trace spectrum at t_1. The red line in the lower plots is the best fit line that determines Q by specifying a limited frequency band where the trace stands out.

(a)

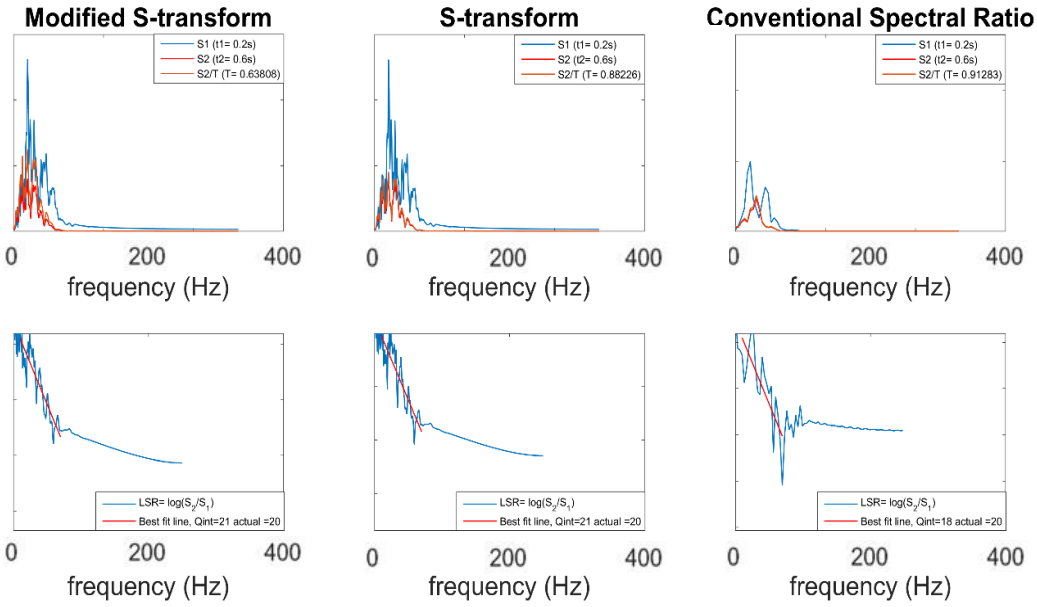

(b)

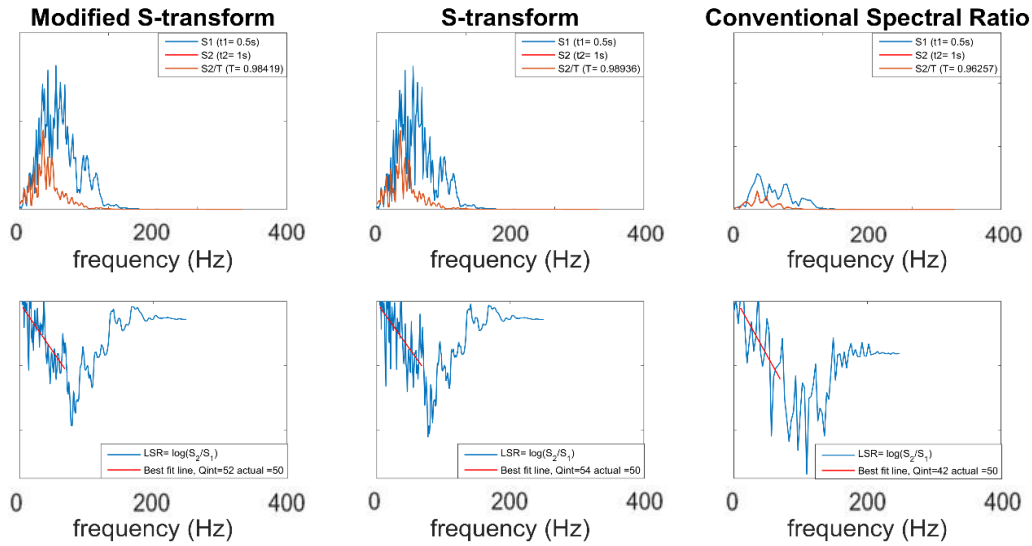

Figure 7. Q estimation for two synthetic traces using the spectral ratio method with the modified S-transform, S-transform and Fourier transform. (a) Q estimation for a synthetic trace with a dominant frequency of 60 Hz and an initial Q of 20 and (b) Q estimation for a synthetic trace with a dominant frequency of 60 Hz and an initial Q of 50. The upper plots are the frequency spectra of the trace at t_1 (blue) and at t_2 (red). The lower plots are the division results of the trace spectrum at t_2 over the trace spectrum at t_1. The red line in the lower plots is the best fit line that determines Q by specifying a limited frequency band where the trace stands out.

(a)

(b)

(c)

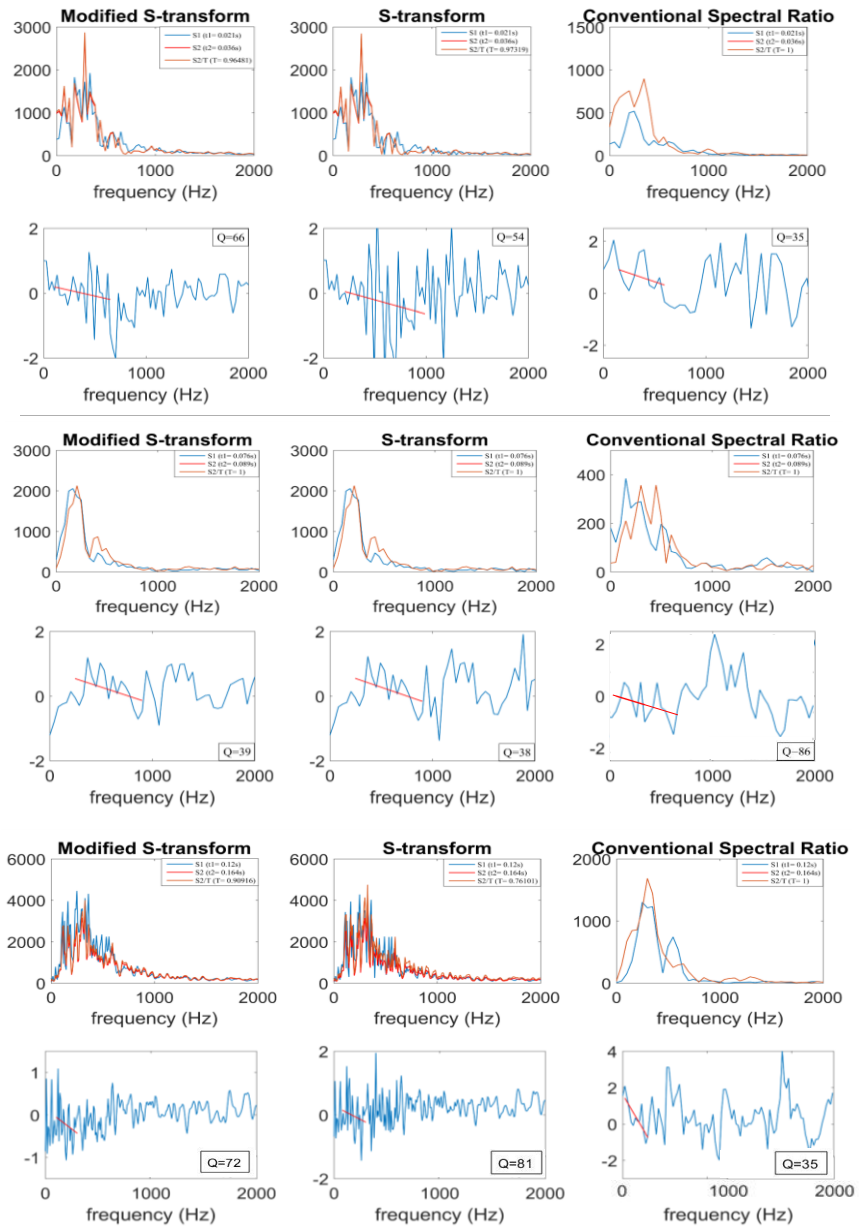

Figure 8. Q estimation for trace 125 (real data) using the spectral ratio method with the modified S-transform, S-transform and Fourier transform. Q estimates for the area above the reef (a), within the reef (b) and below the reef (c). The upper plots are the frequency spectra of the trace at t_1 (blue) and at t_2 (red). The lower plots are the division results of the trace spectrum at t_2 over the trace spectrum at t_1. The red line in the lower plots is the best fit line that determines Q by specifying a limited frequency band where the trace stands out.

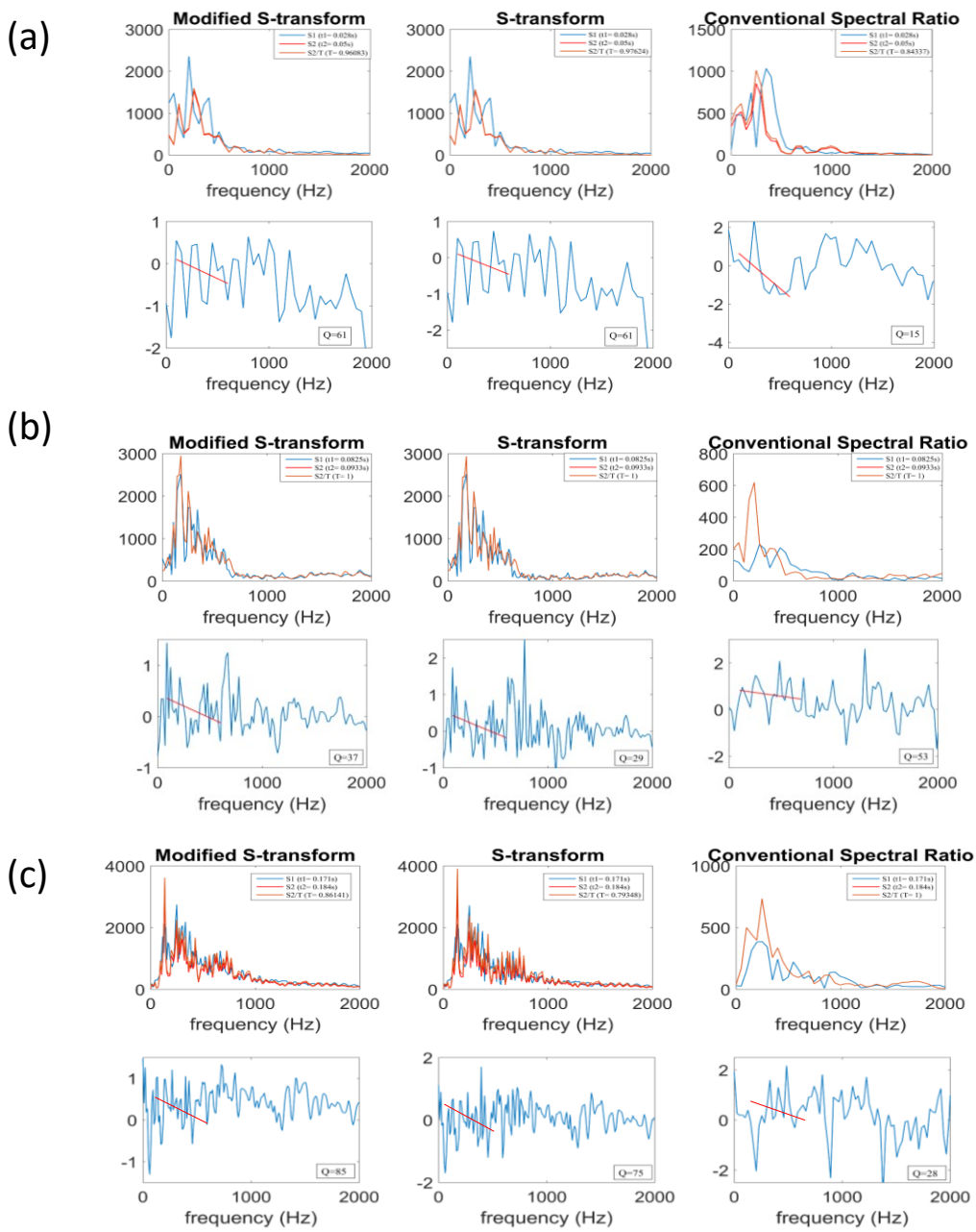

Figure 9. Q estimation for trace 150 (real data) using the spectral ratio method with the modified S-transform, S-transform and Fourier transform. Q estimates for the area above the reef (a), within the reef (b) and below the reef (c). The upper plots are the frequency spectra of the trace at t_1 (blue) and at t_2 (red). The lower plots are the division results of the trace spectrum at t_2 over the trace spectrum at t_1. The red line in the lower plots is the best fit line that determines Q by specifying a limited frequency band where the trace stands out.

5. Conclusion

We assessed the Margrave deconvolution in highly attenuating media using three different time-frequency decomposing methods including the Gabor, S-, and modified S transforms. We find out that when attenuation is high, or the quality factor dramatically varies with depth (as we observed in our field data), the modified S transform is robust over the Gabor and the S transforms. This better achievement is the result of a better time-frequency localization that is obtained from the linear frequency function in the Gaussian window.

We also analyzed the performance of Fourier, S- and modified S transforms in estimating Q using the spectral ratio method. We showed that the spectral decomposing methods which use a frequency dependent window produce Q estimates with more accuracy.

6. References

Askari, R. and Siahkoohi, H. R., 2008, Ground roll attenuation using the S and x-f-k transforms: Geophysical Prospecting, 56, 105-114.

Askari, R. and Ferguson, R. J., 2012, Dispersion and the dissipative characteristics of surface waves in the generalized S-transform domain: Geophysics, 77, V11-V12.

Askari, R., Hejazi, H. S., 2015, Estimation of surface-wave group velocity using slant stack in the generalized S-transform domain: Geophysics, 80, EN83-EN92.

Carrillo, P., Aldana, M., Bryans, B. and Turpening, R, 2007, Attenuation coefficient tomogram and Q distribution image from crosswell survey in the Northern Reef Trend of Michigan Basin: SEG Technical Program Expanded Abstracts .

Du, J., Lin, S., Sun, W., Oilfield, S. and Liu, G, 2010, Seismic attenuation estimation using S transform with regularized inversion: SEG Technical Program Expanded Abstracts.

Gabor, D., 1946, Theory of communication: IEEE (london), 93, 429-457.

Heisenberg, W., 1927, Ueber den anschaulichen Inhalt der quantentheoretischen Kinematik and Mechanik: Zeitschrift für Physik, 43, 172-198. English translation in (Wheeler and Zurek, 1983), pp. 62-84.

Ibrahim, M. S., Pennington, W. D. and Turpening, R. M., 2010, Crosswell seismic imaging of acoustic and shear impedance in a Michigan reef: The Leading edge, 29(6), 706-711.

Jannsen, D., Voss, J. and Theilen, F, 1985, Comparison of methods to determine Q in shallow marine sediments from vertical reflection seismograms: Geophysical Prospecting, 23, 479-497.

Li, D., and Castagna, J., 2013, Modified S-transform in time-frequency analysis of seismic data: SEG Technical Program Expanded Abstracts, 4629-4634.

Margrave, G.F., Lamoureux, M.P., Grossman, J.P., and Iliescu, V., 2002, Gabor deconvolution of seismic data for source waveform and Q correction: SEG Convention expanded abstracts.

Margrave, G.F., Lamoureux, M.P., and Henley, D. C., 2011, Gabor Deconvolution: Estimating reflectivity by nonstationary deconvolution of seismic data : Geophysics, 76, W15-W30.

Margrave, G.F., 1998, Theory of nonstationary linear filtering in the Fourier domain with application to time-variant filtering: Geophysics, 63, 244-259.

Mavko, G., Mukerji, T. and Dvorkin, J, 2009, The Rock Physics Handbook: Cambridge .

Rada, M., Gholami, A., and Siahkoohi, H. R., 2015, S-transform with maximum energy concentration: Application to non-stationary seismic deconvolution: Journal of Applied Geophysics, 118, 155-166.

Reine, C., Baan, M. V. D. and Clark, R, 2009, The robustness of seismic attenuation measurements using fixed- and variable-window time-frequency transforms: Geophysics, 74, WA123-WA135.

Spencer, T.W., J. R. Sonnad, and T. M. Butler, 1982, Seismic Q—Stratigraphy or dissipation: Geophysics, 47, 16–24.

Stockwell, R. G., 2006, A basis for efficient representation of the S-transform: Digital Signal processing, 17, 371-393.

Stockwell, R. G., Mansinha, L., and Lowe, R. P., 1996, Localization of the complex spectrum: The S-trasnform : IEEE Transactions on Signal Processing, 44, 998-1001.

Tonn, R, 1991, The determination of the seismic factor Q from VSP data: A comparison of different computational methods: Geophysical Prospecting, 39, 1-27.

Todorov, T. I. and Margrave, G. F., 2009, Variable factor S-transform seismic data analysis: CREWES Research Report, 21.

Yilmaz, O., 2001, Seismic data analysis: SEG.